

Final results on the neutrino magnetic moment from the MUNU experiment

The MUNU collaboration: Z. Daraktchieva ^a, C. Amsler ^b, M. Avenier ^c, C. Brogгинi ^d, J. Busto ^a, C. Cerna ^d, F. Juget ^a, D.H. Koang ^c, J. Lamblin ^c, D. Lebrun ^c, O. Link ^b, G. Puglierin ^d, A. Stutz ^c, A. Tadsen ^d, J.-L. Vuilleumier ^a, V. Zacek ^e

^aInstitut de physique, A.-L. Breguet 1, CH-2000 Neuchâtel, Switzerland

^bPhysik-Institut, Winterthurerstr. 190, CH-8057 Zurich, Switzerland

^cLaboratoire de Physique Subatomique et de Cosmologie, IN2P3/CNRS-UJF, 53 Avenue des Martyrs, F-38026 Grenoble, France

^dINFN, Via Marzolo 8, I-35131 Padova, Italy

^eUniversité de Montréal, C. P. 6128, Montréal, P.Q. Canada H3C 3J7

The MUNU detector was designed to study $\bar{\nu}_e e^-$ elastic scattering at low energy. The central component is a Time Projection Chamber filled with CF_4 gas, surrounded by an anti-Compton detector. The experiment was carried out at the Bugey (France) nuclear reactor. In this paper we present the final analysis of the data recorded at 3 bar and 1 bar pressure. Both the energy and the scattering angle of the recoil electron are measured. From the 3 bar data a new upper limit on the neutrino magnetic moment $\mu_e^{short} < 9 \cdot 10^{-11} \mu_B$ at 90 % CL was derived. At 1 bar electron tracks down to 150 keV were reconstructed, demonstrating the potentiality of the experimental technique for future applications in low energy neutrino physics.

1. Introduction

The MUNU experiment was designed to study $\bar{\nu}_e e^-$ elastic scattering at low energy and to probe the existence of a magnetic moment of the electron antineutrino. The detector is located at 18 m from the core of a 2.75 GWth commercial nuclear reactor in Bugey (France). The central component is a CF_4 gas Time Projection Chamber (TPC). In [1] we presented an analysis of 66.6 days live time of reactor-on data, as well as 16.7 days of reactor-off data, taken at a pressure of 3 bar. In this Letter we present the final analysis, using the same data set, and the same event selection, but taking better advantage of the electron kinematics, extending the area in which the background is measured and achieving a more precise determination. Moreover we present the analysis of 5.3 days live time of reactor-on data taken at

1 bar pressure.

Technical details of the MUNU detector have already been presented in ref.[2,3]. Here we only describe the most essential features.

2. The experiment

The central part of the detector is a cylindrical TPC filled with CF_4 gas. Measurements were performed at a pressure of 3 bar (11.4 kg of CF_4) and 1 bar (3.8 kg). The gas serves as target and detector medium for the recoil electrons. CF_4 was chosen because of its high density, low atomic number, which reduces multiple scattering, and its absence of free protons, which eliminates the background from $\bar{\nu}_e p \rightarrow e^+ n$. As shown in fig. 1 the gas is contained in a 1 m³ acrylic vessel 90 cm in diameter and 160 cm long. The drift volume is defined on one end by a plain cathode and

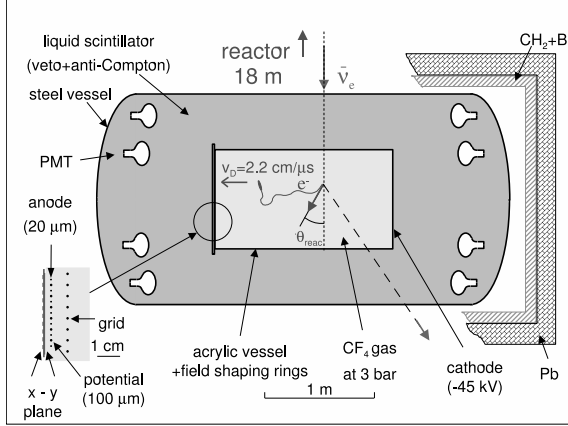


Figure 1. The MUNU detector at the Bugey reactor.

the other one by a grid made from wires. An anode plane made of $20\ \mu\text{m}$ wires with a pitch of $4.95\ \text{mm}$, separated by $100\ \mu\text{m}$ potential wires, is placed behind the grid to collect and amplify the ionization charge. The integrated anode signal gives the total deposited energy. An $x - y$ read-out plane is located behind the anode plane. It contains x strips on one side, and perpendicular y strips on the other one. The pitch is $3.5\ \text{mm}$. The signals induced in these strips provide the spatial information in the x and y directions. The third projection z is obtained from the time evolution of the signal. The drift field was selected such as to achieve a drift velocity of $2.15\ \text{cm}/\mu\text{s}$.

It must be noted that the detector is installed under the reactor core, at an angle of 45° . The detector axis is perpendicular to the reactor core-detector axis. The anode wires are parallel to the reactor core-detector axis, and the grid wires perpendicular to it. The x strips are vertical and the y strips horizontal. The read-out plane is therefore by construction symmetric with respect to four directions: reactor core to detector and opposite, as well as the two orthogonal directions.

The acrylic vessel is immersed in a steel tank ($2\ \text{m}$ diameter and $3.8\ \text{m}$ long), filled with $10\ \text{m}^3$ of liquid scintillator (NE235) and viewed by

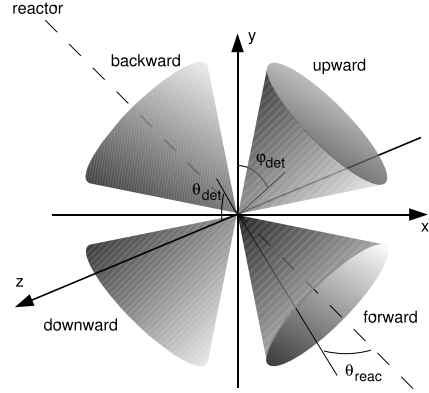


Figure 2. The four kinematical cones.

48 photomultipliers (PMT). The liquid scintillator acts as an anti-Compton detector and as a veto against cosmic muons. The anti-Compton detector also sees the primary scintillation light of heavily ionizing particles such as α 's, and the secondary light emitted during the amplification process around the anode wires, which provides a second measurement of the total deposited energy.

In addition, the detector is shielded against local activities by $8\ \text{cm}$ of boron loaded polyethylene and $15\ \text{cm}$ of Pb. The concrete and steel overburden of the laboratory corresponds to the equivalent of $20\ \text{m}$ of water.

Events in the TPC not in coincidence with a signal above $22\ \text{MeV}$ in the scintillator within an $80\ \mu\text{s}$ time window are recorded. The selection of good events off-line proceeds in two steps. First a software filter rejects the muon related events, Compton electrons, discharges and uncontained events. The selection is finalized in a visual scan. A neutrino scattering candidate event is a continuous single electron track fully contained in a $42\ \text{cm}$ fiducial radius, with no energy deposition above $90\ \text{keV}$ in the anti-Compton in the preceding $200\ \mu\text{s}$. The initial direction of the electron track is obtained from a visual fit [1]. The scattering angles in the x - z and y - z projections are determined first, and used to calculate the

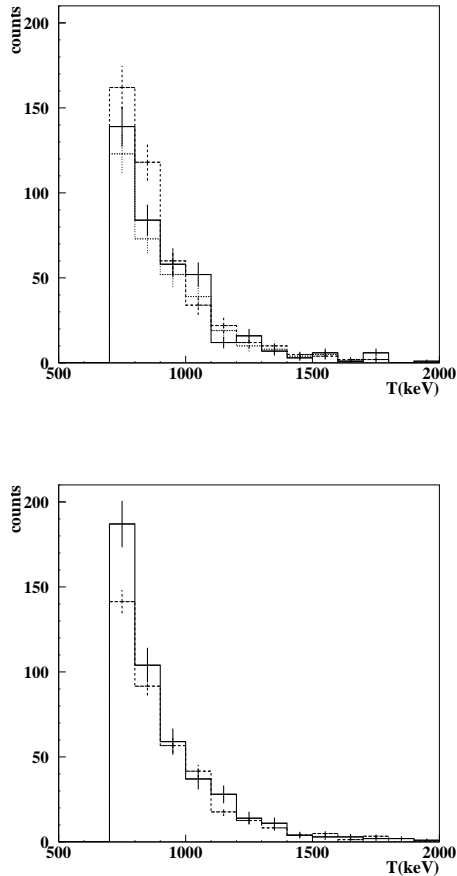


Figure 3. 3 bar data, reactor-on, energy spectra; top: upward (dashed line), downward (solid line) and backward (dotted line) electrons; bottom: forward (solid line) and NB (dashed line) electrons

scattering angle θ_{reac} with respect to the reactor-detector axis, which coincides quite precisely with the scattering angle, as well as the angle θ_{det} with respect to the detector axis (see fig.2). The angle φ_{det} between the projection of the initial track direction on the x-y plane and the vertical y axis is also determined.

As described in more details in [1] we apply the angular cut $\theta_{det} < 90^\circ$ to suppress the background from activities on the read-out plane side of the TPC, which was found to be noisier. This is presumably due to the greater complexity of

the anode side and the larger inactive volume in the scintillator.

The reactor neutrino spectrum, necessary to interpret the data, was calculated using the formalism described in [1,4]. Above 1.5 to 2 MeV neutrino spectra reconstructed from the measured β spectra of the fission fragments were used. The uncertainty is of order 5 % or less in this energy range, in which the neutrino spectrum was moreover thoroughly probed in measurements of $\bar{\nu}_e p \rightarrow e^+ n$ scattering at reactors. At lower energies calculations only are available. We have used the calculated neutrino spectra of the fission fragments from [5,6], and taken into account the neutron activation of ^{238}U , as discussed in [7], which is significant below 1 MeV. The uncertainty in the neutrino spectrum in this energy range was estimated to 20 %.

3. 3-bar forward-normalized background analysis

The 3 bar data were taken with a TPC trigger threshold of 300 keV. Considering the entire event selection procedure, the live time, limited primarily by the data transfer rate and the anti-Compton, was 65 %. At 3 bar the tracks are long enough to be scanned with sufficient efficiency for electron kinetic energies $T_e > 700$ keV. As before we rely on kinematics to select the good candidate events. For each electron track the neutrino energy E_ν is reconstructed from the scattering angle, taken as θ_{reac} , and the measured electron recoil energy T_e . Events with $E_\nu > 0$ are declared forward events since, effectively, this criteria selects electrons with an initial track direction within a forward cone, the axis of which coincides with the reactor core-detector axis. The opening angle depends on the energy, and is larger than that of the kinematic cone for recoil electrons ($E_\nu > T_e$). Simulations taking into account the angular response of the detector show that nearly 100 % of the recoil electrons fall in the forward category, which however also contains a contribution from the background, which is isotropic around the detector axis.

To estimate the background the same procedure is applied in the three directions equiva-

lent, considering the read-out plane, to the reactor core-detector direction, taken as reference for the forward events. These directions are thus also equivalent from the point of view of the angular response in φ_{det} , which is not completely linear, and of the acceptance. As depicted in fig.2 these directions define the backward cone, opposite to the forward cone, and the two perpendicular upward and downward cones [8]. To avoid overlap of the cones, which can occur for $T_e < 2m_e c^2$, we require in addition that the angle φ_{det} is within less than 45° with respect to the cone axis. This only reduces the acceptance of the forward cone for recoil electrons in a negligible way.

While the forward electrons contain recoil plus background events, the backward, upward and downward electrons are background events only. The energy distributions of the upward, downward and backward electrons (1154 ± 34 in total) are presented in fig. 3. The distributions are compatible within the errors, which confirms the isotropy of the background inside the TPC.

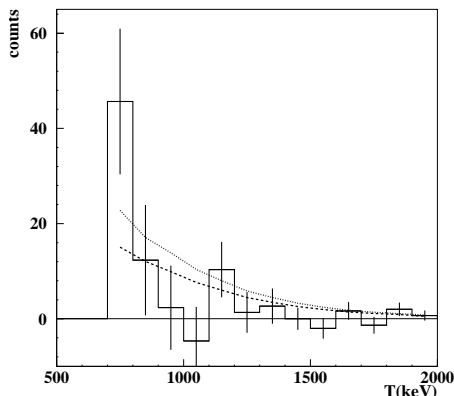


Figure 4. Energy distribution of the forward minus NB electrons above 700 keV, 3 bar, reactor-on; comparison with the expected spectrum for weak interaction alone (dashed line) and for a magnetic moment of $9 \cdot 10^{-11} \mu_B$ (dotted line).

We normalize the background to the forward cone by dividing by 3 the rates in the backward, upward and downward cones. This normalized

background (NB) is then directly compared with the event rate in the forward cone. The energy distributions of both forward (455 ± 21) and NB (384 ± 11) electrons are shown in fig.3. There is a clear excess of forward events, from the reactor direction. The total number of events forward minus NB above 700 keV is 71 ± 23 counts for 66.6 days live time reactor-on, corresponding to 1.07 ± 0.34 counts per day (cpd). The forward minus NB spectrum representing the measured electron recoil spectrum is displayed in fig. 4.

We make the same analysis with the data taken during the reactor-off period as a cross check (16.7 days live time). The energy distributions of both forward (133 ± 11) and NB electrons (147 ± 7) are given in fig.5. The integrated forward minus NB rate above 700 keV is -0.8 ± 0.8 cpd, consistent with zero.

We now turn to the comparison with expectations. Monte Carlo simulations (GEANT 3) were used to calculate the various acceptances of the event selection procedure. The detector containment efficiency in the 42 cm fiducial radius was found to vary from 63 % at 700 keV, 50 % at 1 MeV to 12 % at 2 MeV, with a typical error of 2 %. The errors on the global acceptance, including track reconstruction efficiency (4 %), are of order of 7 %. This leads to an expected event rate above 700 keV of 1.02 ± 0.10 cpd assuming a vanishing magnetic moment. This is in good agreement with the observed 1.07 ± 0.34 cpd.

The measured and expected recoil spectra for no magnetic moment are compared in fig.4. First we note that the large excess of events in the first two bins (700- 900 keV) observed in our previous analysis [1] has to a large extent disappeared. It is thus most likely due to a statistical fluctuation in the background, more precisely determined in the present analysis. And second the measured and expected spectra are seen to be in agreement.

For a more quantitative analysis the χ^2 method was used as in [1], with the same binning for Gaussian statistics to apply (100 keV bins from 700 keV to 1400 keV, and then a bin from 1400 to 2000 keV). The magnetic moment is varied to find the best fit. We remind that the neutrinos travel over a short distance only so that the experiment probes the magnetic moment μ_e^{short} ,

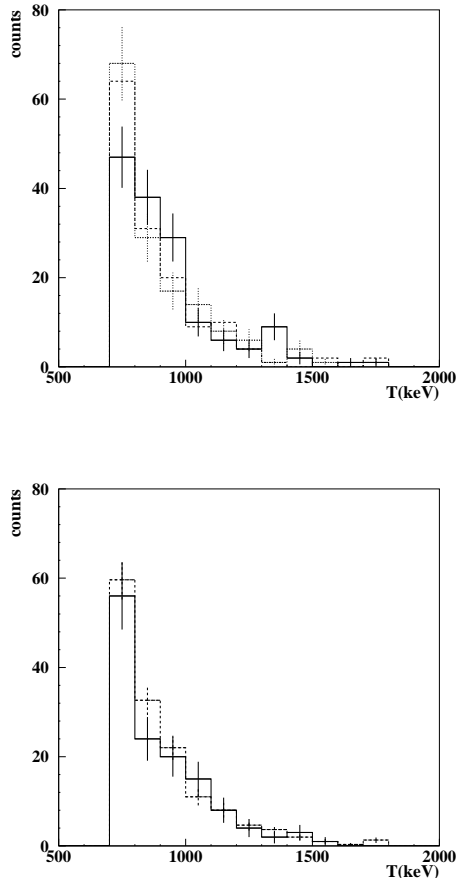


Figure 5. 3 bar data, reactor-off, energy spectra; top: upward (dotted line), downward (solid line) and backward (dashed line) electrons; bottom: forward (solid line) and NB (dashed line) electrons

as described in ref. [1], to be precise its square. The allowed range at the 90 % CL is $(\mu_e^{short})^2 = (-0.72 \pm 1.25) \cdot 10^{-20} \mu_B^2$, with $\chi^2=11.5$ for 7 degrees of freedom at the central value. This result is compatible with a vanishing magnetic moment. To obtain a limit on μ_e^{short} we renormalize to the physical region ($(\mu_e^{short})^2 > 0$) and obtain $\mu_e^{short} < 9(7) \cdot 10^{-11} \mu_B$ at 90(68) % C.L. This constitutes a small improvement over our previous analysis [1], restricted to recoil energies above 900 keV. The improvement results from the lower threshold and the better background estimation.

We can compare this with results from other experiments. The TEXONO collaboration is performing an experiment near the Kuo-Sheng reactor in Taiwan [9]. Thanks to the use of an Ultra Low Background High Purity Germanium detector they achieve a very low threshold of 12 keV. The reactor-on minus reactor-off rates were found to be identical and from that the limit $\mu_e^{short} < 1.3 \cdot 10^{-10} \mu_B$ at 90 % C.L was deduced. Superkamiokande [10,5] reported the limit $\mu_e^{sol} < 1.5 \cdot 10^{-10} \mu_B$ at 90 % CL from the study of the shape of the recoil spectrum of electrons in the scattering of solar neutrinos. Depending on oscillation parameters, this quantity may however differ from μ_e^{short} .

4. 1-bar forward-normalized background analysis

The technical details of the 1 bar measurements will be presented elsewhere. Here we restrict ourselves to the most relevant parameters. The trigger threshold on the electron recoil was lowered to 100 keV. The trigger rate is 0.4 s^{-1} . The dead-time, here also mostly due to the data read-out and transfer time, and to the anti-Compton, is around 50 %, somewhat less than for the measurements at 3 bar. The energy calibration of the TPC is again determined with ^{137}Cs and ^{54}Mn radioactive sources. The energy resolution is found to vary from 10 % (1σ) at 200 keV to 6 % at 600 keV following an empirical $E^{0.57}$ law. Data were accumulated during 5.3 days live time reactor-on.

The selection of good events proceeds in two steps, as with the 3 bar data, ending with a visual scan. Tracks can be reconstructed with reasonable efficiency for energies above 150 keV. Events above that energy are retained. As an example a 190 keV electron track in 1 bar of CF_4 is shown in fig.6. The end of the track is easily identified from the increased energy deposition (blob). The containment efficiency of the TPC in the 42 cm fiducial radius for recoil electrons was calculated with the GEANT3 simulation code, and found to vary from 85 % at 200 keV, 50 % at 400 keV to 5 % at 1 MeV. The angular resolution was determined by scanning visually simulated electron tracks. It varies from 15° (1σ) at 200 keV, 12°

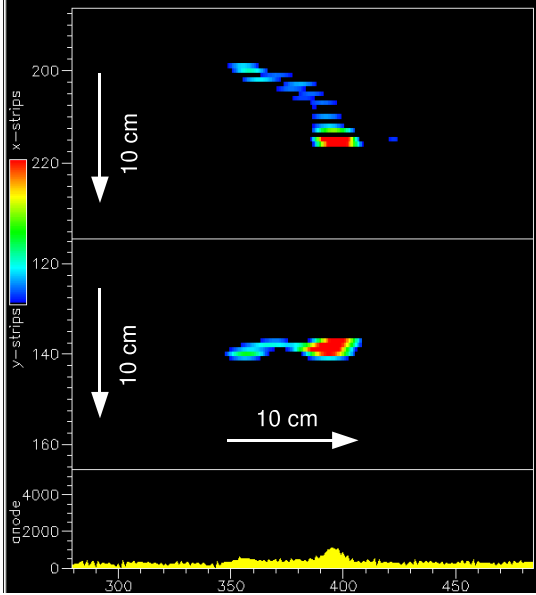


Figure 6. A 190 keV electron at 1 bar in the TPC; the xz, yz projections are displayed as well as the anode signal.

at 400 keV, to 10° above 500 keV.

The angular cut $\theta_{det} < 90^\circ$ is also applied in the 1 bar analysis. The electrons are selected in the same four kinematical cones. Here however the overlap of the cones is more critical. The constraint in φ_{det} is done somewhat differently: downward electrons 190° to 270° , forward electrons 80° to 190° , upward electrons 0° to 80° and backward electrons 270° to 0° .

This makes the solid angle for the forward electrons somewhat larger. We expect from the Monte Carlo simulations that nearly 100 % of the recoil events above 200 keV will fall in it. The normalized background NB in the three other cones has to be scaled accordingly, with a factor which remains close to 3 however. The energy distributions of the upward, downward and backward electrons (326 ± 18 in total) are presented in fig.7. They are seen to be compatible within the errors.

The energy distributions of the forward (124 ± 11) and NB (109 ± 6) electrons are displayed in fig. 7. The difference is 15 ± 12 events, giv-

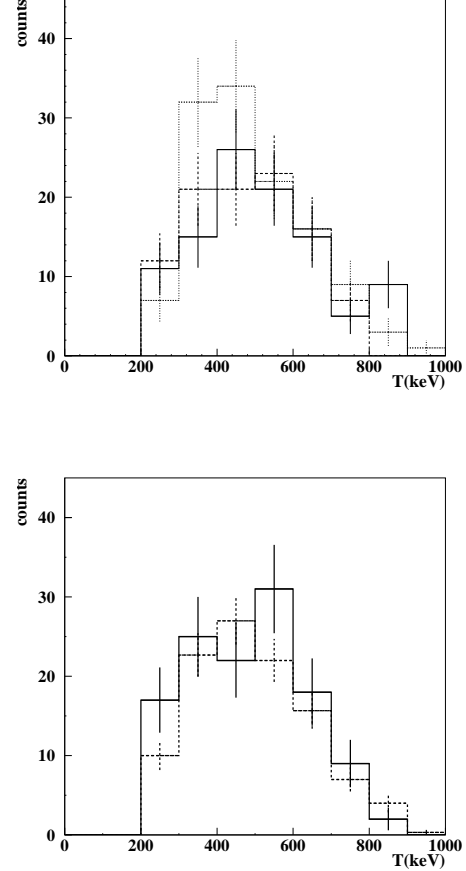


Figure 7. 1 bar data, reactor-on, energy spectra; top: upward (dotted line), downward (solid line) and backward (dashed line) electrons; bottom: forward (solid line) and NB (dashed line) electrons

ing an indication of a signal, corresponding to 2.89 ± 2.39 counts per day. The energy distribution is shown in fig.8. This measured total rate above 200 keV agrees with the expected value 0.49 ± 0.12 counts per day, assuming no magnetic moment. The error comes mainly from the uncertainties in the low energy part of the neutrino spectrum, as described above. Due to the limited statistics the data do not have a competitive sensitivity to the neutrino magnetic moment. Nevertheless our experiment shows that a gas TPC can be used to measure the energy and direction

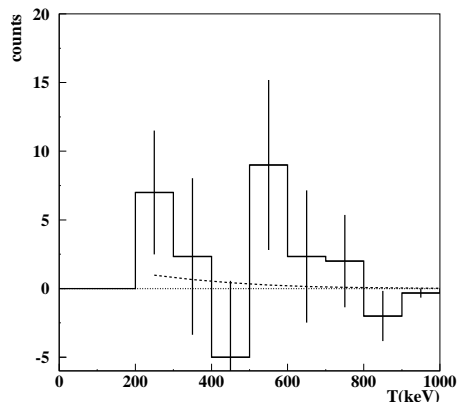


Figure 8. Energy distribution of the forward minus NB electrons above 200 keV, 1 bar, reactor-on; comparison with the expected spectrum for weak interaction alone (dashed line).

of electrons with energies as low as 150 keV. Provided background problems can be solved, this opens the way, for instance, to on-line measurements of low energy solar neutrinos from the pp reaction.

5. Conclusions

The MUNU experiment studied $\bar{\nu}_e e^-$ scattering at low energy near a nuclear reactor, measuring both the energy and scattering angle of the recoil electron. Thanks to a better estimation of the background in a larger kinematical domain it was possible to reduce the statistical uncertainties, analyzing data taken at 3 bar of CF_4 during 66.6 days live time reactor-on with an energy threshold of 700 keV. Good agreement is observed between the measured and expected recoil spectra assuming weak interaction alone. From this the limit on the neutrino magnetic moment $\mu_e^{short} < 9 \cdot 10^{-11} \mu_B$ at 90 % CL was derived. Moreover reactor-on data were taken at 1 bar of CF_4 during 5.3 days live time. Electron tracks were reconstructed efficiently down to 150 keV recoil energy. This demonstrates the potentiality of gas TPC's for possible future applications in low energy neutrino physics.

The authors want to thank the directors and

the staff of EDF-CNPE Bugey for the hospitality. This work was supported by IN2P3, INFN, and SNF.

REFERENCES

1. The MUNU Collaboration, Z. Daraktchieva, et al., Phys. Lett. B 564 (2003) 190
2. The MUNU Collaboration, C. Amsler, et al., Nucl. Inst. Meth. A 396 (1997) 115.
3. The MUNU collaboration, M. Avenier et al., Nucl. Inst. and Meth. A482 (2002) 408
4. G. Zacek et al., Phys. Rev. D34 (1986) 2621
5. J. F. Beacom and P. Vogel, Phys. Rev. Lett. 83 (1999) 5222
6. P. Vogel and J. Engel, Phys. Rev. D39 (1989) 3378
7. V.I. Kopeikin et al. Phys. of Atomic Nuclei Vol. 60 (1997) 172
8. Z. Daraktchieva, Thesis, University of Neuchatel, 2004
9. The TEXONO collaboration, H. B. Li, et al., Phys. Rev. Lett. 90 (2003) 131802.
10. The SuperKamiokande collaboration (Y. Fukuda et al., Phys. Rev. Lett. 82 (1999) 2430

